

Biphasic Janus particles with nanoscale anisotropy

KYUNG-HO ROH¹, DAVID C. MARTIN^{1,2} AND JOERG LAHANN^{1,2,3*}

¹Macromolecular Science and Engineering Center, The University of Michigan, 48109 Ann Arbor, Michigan, USA

²Department of Materials Science and Engineering, The University of Michigan, 48109 Ann Arbor, Michigan, USA

³Department of Chemical Engineering, The University of Michigan, 48109 Ann Arbor, Michigan, USA

*e-mail: lahann@umich.edu

Published online: 25 September 2005; doi:10.1038/nmat1486

Advances in the field of nanotechnology have fuelled the vision of future devices spawned from tiny functional components that are able to assemble according to a master blueprint¹. In this concept, the controlled distribution of matter or ‘patchiness’² is important for creating anisotropic building blocks and introduces an extra design parameter—beyond size and shape^{3,4}. Although the reliable and efficient fabrication of building blocks with controllable material distributions will be of interest for many applications in research and technology, their synthesis has been addressed only in a few specialized cases^{5,6}. Here we show the design and synthesis of polymer-based particles with two distinct phases. The biphasic geometry of these Janus particles is induced by the simultaneous electrohydrodynamic jetting^{7–9} of parallel polymer solutions under the influence of an electrical field. The individual phases can be independently loaded with biomolecules or selectively modified with model ligands, as confirmed by confocal microscopy and transmission electron microscopy. The fact that the spatial distribution of matter can be controlled at such small length scales will provide access to unknown anisotropic materials. This type of nanocolloid may enable the design of multicomponent carriers for drug delivery, molecular imaging or guided self-assembly.

Work in the area of electrohydrodynamics has resulted in isotropic materials made from single-phase polymer solutions^{9–13}, blends¹⁴ and hybrid materials^{15–17}, as well as coaxial fibres^{16,17} and core/shell particles^{17–20}. In response to the applied electrical field, the liquid drop at the tip of the nozzle is distorted into a narrow cone (the Taylor cone)⁷. The electrical field further induces a stretching process that leads to the formation of a nanometre-thick polymer thread, which—in conjunction with solvent evaporation—accounts for most of the size reduction.

During our electrohydrodynamic processing experiments, a laminar flow of two distinct polymer solutions was pumped at suitable flow rates, typically in the range of $\mu\text{l min}^{-1}$, through a modified nozzle with side-by-side geometry (Fig. 1a)^{21,22}. The side-by-side geometry was selected over coaxial geometries^{16–20}, because of the bipolar polymer/polymer interface that was maintained between two jetting fluids throughout the nozzle until electrified

jetting occurred. Figure 1b shows a micrograph of the outlet region of the nozzle. In this setup, the biphasic character of the jetting liquid continued throughout the droplet (Fig. 1a) and resulted in a single liquid thread that was formed at the interface of the two jetting solutions. Under certain conditions (polyethylene oxide, PEO, solutions in distilled water), we observed a vortex at the tip of the liquid cone (Fig. 1b, inset). The spontaneous formation of vortices has been observed during electrified jetting of organic solvents²³ that had substantially lower viscosities ($<10\text{ mPa s}$) and electrical conductivities ($0.5\ \mu\text{S cm}^{-1}$; ref. 23) than the aqueous polymer solutions used in this study (see Supplementary Information, Table S1). The formation of the vortex was reproducible and did not seem to interfere with the actual synthesis of biphasic particles. In our jetting experiments, the liquid jets ejected from a Taylor cone could either be fragmented into particles or sustained and elongated in the form of continuous fibres. As reported for one-phasic systems^{10–12}, the differences in the final morphologies were mainly determined by properties of the jetting liquids (viscosity, conductivity and surface tension) and electrohydrodynamic parameters (applied field strengths, flow rates), and could be controlled with relative ease.

One objective of our initial experiments was to determine whether biphasic particles with sub-micrometre diameters are accessible through electrohydrodynamic jetting. In a series of experiments, we fabricated biphasic objects from a dilute aqueous solution of a PEO ($M_w = 600,000\ \text{g mol}^{-1}$). The morphology of the objects was characterized by transmission electron microscopy (TEM). Depending on the choice of process parameters, the shape of the objects was varied and both discontinuous particles and long fibres could be observed. Figure 2a and b shows characteristic TEM micrographs of biphasic particles prepared from two jetting fluids: (i) 1% (weight per volume, w/v) PEO and 1.5% w/v sodium polystyrene sulphonate (PSS, $M_w = 200,000\ \text{g mol}^{-1}$); and (ii) 1% w/v PEO and 0.9% w/v polyethylene imine (PEI, $M_w = 750,000\ \text{g mol}^{-1}$). PSS, characterized by the dark contrast in TEM images, was selectively found in one phase revealing the biphasic character. Most of the polyethylene oxide-based objects had diameters between 100 and 400 nm and were connected through nanofibres with approximate diameters below 10 nm.

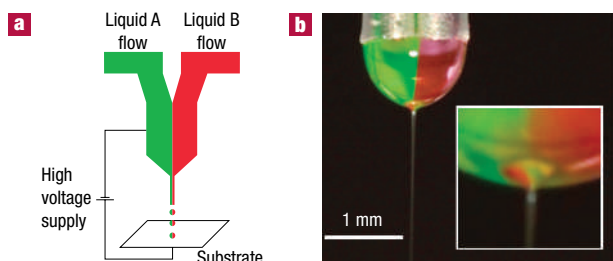


Figure 1 Biphasic electrified jetting using side-by-side dual capillaries.

a, A schematic diagram of the experimental setup used for electrohydrodynamic processing. When exposed to an applied electric potential (5–15 kV depending on the jetting conditions), the bipolar jetting liquid experiences an electrical field that is formed between the tip of the liquid and the counter-electrode (collecting substrate). For certain parameter combinations, well-structured biphasic Taylor cones were observed at the tip of the nozzle, consisting of two aligned fluid phases. **b**, A digital image of a typical biphasic Taylor cone with jet. PEO ($M_w = 600,000 \text{ g mol}^{-1}$) dissolved in distilled water (2% w/v) was used in both jetting fluids. Each phase was labelled by addition of 0.5% w/v of a fluorescent dye, that is, fluorescein isothiocyanate-conjugated dextran (green) and rhodamine-B-conjugated dextran (red). The inset shows a detailed image of the swirl-like jet ejection point. The formation of the vortex was reproducible and did not seem to interfere with the actual synthesis of the biphasic particles.

In the case of polyacrylic acid (PAA, $M_w = 250,000 \text{ g mol}^{-1}$, 10% w/v), discontinuous particles as small as 170 nm were observed. Because our Janus particles are larger than traditional nanoparticles^{3–6}, but smaller than typical colloids, we will refer to them as nanocolloids.

Although potential shapes of biphasic nanocolloids are largely unknown, modelling studies may provide means to estimate what stable structures can be expected²⁴. During electrohydrodynamic jetting, nano-objects emerge from fluid droplets with predictable geometries. At equilibrium, a fluid droplet composed of a phase A and a phase B has three characteristic free surface energies: the surface free energy of the phase A/vapour interface (γ_{AV}), the surface free energy of the phase B/vapour interface (γ_{BV}) and the surface free energy of the phase A/phase B interface (γ_{AB}). For our experimental system, γ_{AV} is similar to γ_{BV} and the equilibrium geometry of the resulting biphasic nanodroplets will mainly be determined by γ_{AB} and the relative volumes (V) of the phases A and B. For $\gamma_{AB} = 0$ and equal amounts of A and B, the equilibrium state is a sphere, with phase A in one hemisphere and phase B in the other. With increasing γ_{AB} , the sphere pinches down in the middle to reduce the interfacial area between phases A and B. This creates a bicomponent particle with a peanut-like geometry (Fig. 2c). For nanodroplets with different volumes of phases A and B, eyeball-like envelopes are formed (Fig. 2d). Figure 2e shows an example of a stable biphasic structure for $\gamma_{AB} = 0$. To a first approximation ($\gamma_{AB} \geq 0$), particle envelopes and interfaces of modelled nanodroplets and particles realized in practice (Fig. 2a,b) were in good agreement. It can therefore be assumed that the predicted structures establish thermodynamic energy minima towards which the nanocolloids will tend to converge during electrified jetting. Nonetheless, the TEM pictures also reveal some differences. For instance, the peanut-like structure of Fig. 2c was not realized in practice, which may indicate that the particles were indeed not fully converged into the equilibrium shape. Observed discrepancies between model and experiment can be attributed to the contribution of extra factors, such as solidification owing to solvent loss or fluid relaxation during electrohydrodynamic processing.

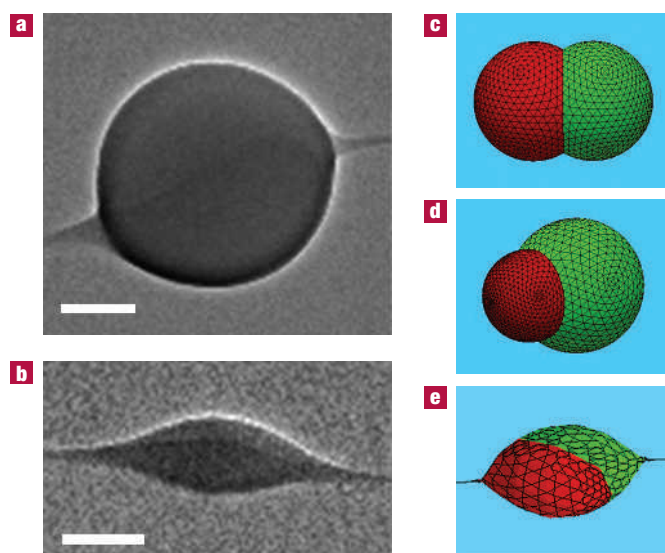


Figure 2 Biphasic anisotropy examined by TEM and modelling. **a, b**, Typical TEM images of biphasic colloids. The jetting solution is composed of 1.0% w/v of PEO ($M_w = 600,000 \text{ g mol}^{-1}$) in each side. In both TEM images, dark contrast was due to PSS (Aldrich, USA), which was included in one jetting solution. PEI (Aldrich, USA) was added to the other jetting solution. The scale bar is 100 nm. **c–e**, Particle morphologies shown for the case that two jetting liquids reach the thermodynamic equilibrium state. For $\gamma_{AV} \approx \gamma_{BV}$, a peanut-like geometry (**c**, $V_A = V_B$ and $\gamma_{AB} > 0$) or an eyeball-like geometry (**d**, $V_A = 4V_B$ and $\gamma_{AB} > 0$) can be obtained; a spindle-like geometry (**e**, $V_A = V_B$ and $\gamma_{AB} = 0$) was obtained by enforcing boundary conditions that tether the two halves of the droplet between two opposing solid surfaces.

On the basis of the results of simulation and experiment, we concluded that: (i) the overall shape of the biphasic nanocolloids resembles shapes previously observed for single-phasic nanoparticles^{10–13}; (ii) preferential compartmentalization is due to the manipulations of the liquid phase and the interface is maintained throughout jetting and solidification; and (iii) the nano-objects represent solidified intermediates. The apparent divergence from the equilibrium shape may provide opportunities to extend the method to the fabrication of biphasic particles with a wide range of non-equilibrium shapes, but may also be a potential source of inhomogeneities in nanocolloid geometries. So far, these phenomena have only been studied for water-based systems and further studies are warranted to establish the limits of these correlations, especially for systems that use organic solvents with lower surface free energies.

Some applications may require particles to act as selective carriers for two or more independent ingredients, such as molecular probes or drugs. To address the question of whether electrohydrodynamic jetting can be used to create Janus particles that can function as multicomponent carriers, we loaded the jetting fluids with two different model molecules, with one in each phase. Using confocal laser scanning microscopy (Fig. 3a,b), both molecules were identified on the basis of their characteristic fluorescence emissions: (i) fluorescein-isothiocyanate- (FITC) labelled dextran (green fluorescence); and (ii) rhodamine-B-labelled dextran (red fluorescence). The confocal micrographs suggest that the two macromolecules preferentially compartmentalized within the particles. This finding was independent of whether we used PEO or PAA as base polymer. The superposition of the images in Fig. 3a,b indicates the biphasic character of the particles along a thin interface that appears yellow in the

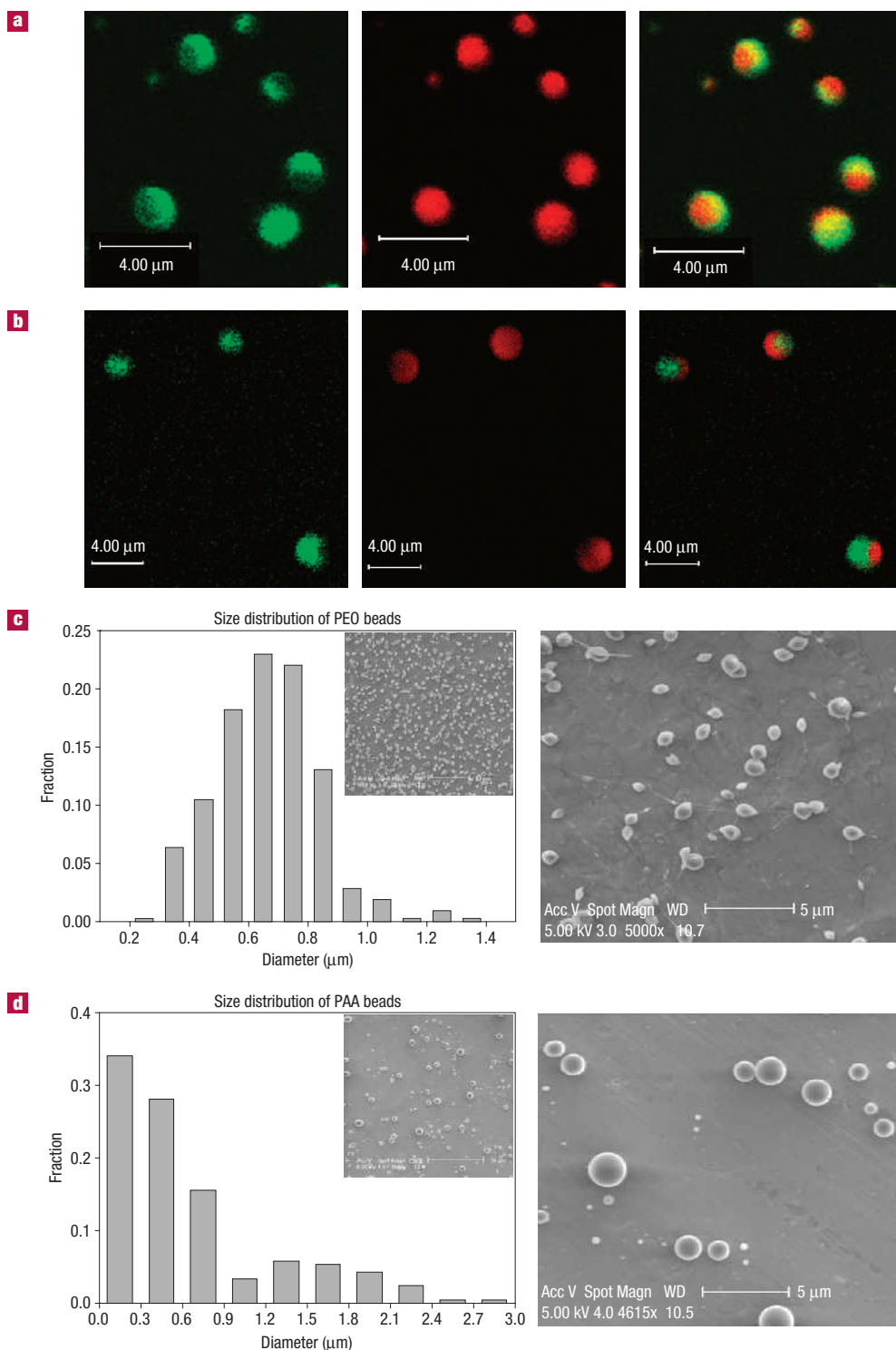


Figure 3 Encapsulation of biomolecules in a dipolar fashion. Two distinct polymer systems based on PEO (**a,c**) and PAA (**b,d**) were used as biphasic carriers. Colour-encoded biomolecules (FITC-dextran, green, and rhodamine-B-dextran, red) were incorporated in individual sides. **a, b**, Confocal micrographs of biphasic particles shown at the fluorescence emission range of FITC and rhodamine B. The overlays of these two phases reveal the biphasic character of the nanocolloids. For confocal microscopy, particles with diameters above 1 μm were selected for best imaging results. **c,d**, Size distributions of PEO (**c**) and PAA (**d**) biphasic particles determined from the SEM images (shown as insets). Typical SEM images of higher magnifications show that PEO particles are linked with fine fibres (beads-on-a-string), whereas PAA particles have almost perfectly spherical envelopes.

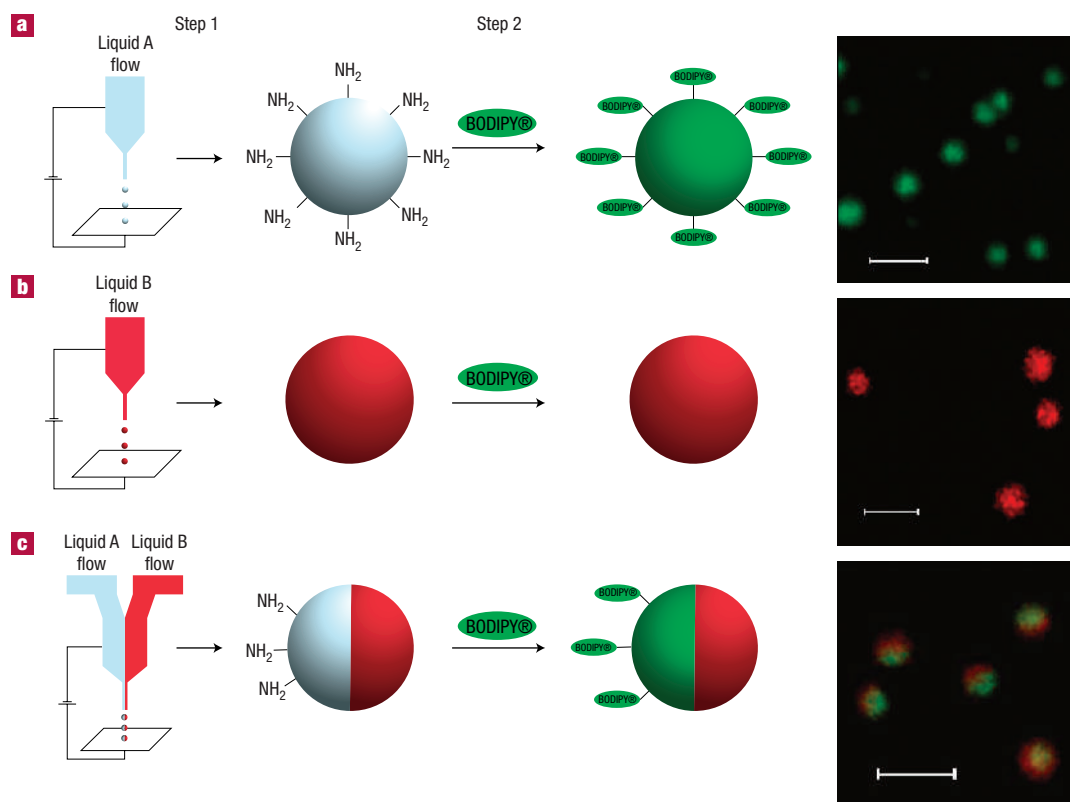


Figure 4 Selective chemical modification. Jetting liquid A is a mixture of PEO ($M_w = 600,000 \text{ g mol}^{-1}$, 2% w/v) and amino-dextran ($M_w = 500,000 \text{ g mol}^{-1}$, 0.5% w/v) dissolved in distilled water. In jetting liquid B, rhodamine-B-dextran ($M_w = 700,000 \text{ g mol}^{-1}$, 0.5% w/v) is used instead of amino-dextran. Confocal images are overlays of green and red fluorescence emission images. **a**, A single jetting experiment with liquid A. The surface is modified by the reaction between amine groups and BODIPY dye molecules. **b**, A single jetting experiment with liquid B. Only red fluorescent is observed owing to rhodamine B originally incorporated in the jetting solution. No fluorescence owing to BODIPY is detected. **c**, Selective chemical modification of one side of the biphasic nanoparticles. Both green fluorescent emission owing to reacted BODIPY dye and red fluorescent emission owing to incorporated rhodamine B are observed, and they reveal the biphasic character of the nanocolloids. The data confirm that the reaction of the biphasic particles with the BODIPY ligand results in selective binding to only one phase. For confocal microscopy, particles with diameters around $1 \mu\text{m}$ were selected for best imaging results. All scale bars are $2 \mu\text{m}$.

confocal micrographs. The particles were further examined by scanning electron microscopy to determine particle shapes and sizes (Fig. 3c,d). Particles made of PEO were spindle-like and had an average diameter of 660 nm and a relatively narrow size distribution (standard deviation: 180 nm), whereas PAA particles had almost perfectly spherical envelopes and were discontinuous. Analysis of the histogram (Fig. 3d) revealed a broader size distribution for PAA nanocolloids. A large subpopulation of the PAA particles consisting of about 80% of all nanocolloids was smaller than $1 \mu\text{m}$ in diameter. For this subpopulation, the average diameter was $(402 \pm 209) \text{ nm}$. It has been shown that hydrodynamic focusing can greatly improve the monodispersity of colloids^{20,25,26}, although less is known for submicrometre-sized particles¹⁹. Nevertheless, the implementation of similar refinements may lead to biphasic nanocolloids with narrower size distributions.

Once the ability of biphasic particles to act as carriers for several components was demonstrated, we directed our study towards the selective modification of one specific particle phase. Selective modification, that is, the ability to independently address only one of the two phases, will result in biphasic particles with distinct surface properties. The enhanced anisotropy, in turn, will be essential to a directed assembly of hierarchical structures or devices (controlled patchiness). This type of selective chemical

modification will also be instrumental in the use of biphasic particles in targeted drug delivery.

To elucidate the possibility of selective modification of patches of the biphasic nanocolloids, we conducted a series of experiments, wherein we added a small amount of an amino-functionalized polymer to one of the jetting fluids before electrohydrodynamic processing. In the example shown in Fig. 4a, single-phasic nanocolloids were prepared by electrohydrodynamic processing of solutions composed of PEO ($M_w = 600,000 \text{ g mol}^{-1}$, 2% w/v) and amino-dextran ($M_w = 500,000 \text{ g mol}^{-1}$, 0.5% w/v). The free amine groups of the resulting particles were subsequently modified with 4,4-difluoro-5,7-dimethyl-4-bora-3a,4a-diaza-s-indacene-3-propionic acid, succinimidyl ester (BODIPY) ligands following a modified reaction protocol developed for conjugation and immobilization of biomolecules²⁷. After chemical modification, the amino-modified nanocolloids showed homogeneously distributed green fluorescence indicating efficient binding of the ligand throughout the entire particle. In a second series of experiments, the nanocolloids were loaded with a rhodamine-dextran instead of the amino-dextran. After modification with BODIPY, no fluorescence associated with the BODIPY ligands was observed, suggesting that unspecific binding of the ligands to the nano-objects did not occur. In contrast, red fluorescence caused by the

rhodamine-dextran was found throughout the reference particles (Fig. 4b). We concluded from these results that the amino groups were available for selective modification through amide formation and that the binding was of covalent nature, rather than based on unspecific interactions. We finally prepared biphasic nanocolloids with an amino-dextran in the first phase and a rhodamine-dextran in the second phase. After reaction with the BODIPY ligand, nanocolloids were examined by confocal microscopy. The resulting micrographs (Fig. 4c) confirm selective binding of the BODIPY ligand to the amino-dextran-containing phase only.

The concept of using small-scale fluid manipulation to fabricate solid materials with properties that are otherwise difficult to obtain has started to emerge as a promising theme in materials processing^{19,25,26}. We have now extended this concept to the fabrication of anisotropic Janus particles. Larger, colloidal Janus particles²⁸ accessible through dewetting²⁹, microcontact printing³⁰ or gel trapping²⁸ have been studied because of their potential as photonic crystals or electrolyte sensitive gels. To fabricate biphasic nanocolloids, we used an electrohydrodynamic jetting process that may be compatible with a wide range of commodity polymers⁹. Future research may be directed towards enhancement of the bipolarity of the particles, improved monodispersity and the development of alternative anisotropic geometries including multiphase nano-objects. The fact that nanocolloids with controlled distributions of matter have been created raises hope that these findings will, with further study, have implications in drug delivery, molecular imaging, electro-rheological fluids and the fabrication of smart displays.

METHODS

MATERIALS AND PREPARATION OF JETTING SOLUTIONS

PEO ($M_w = 600,000 \text{ g mol}^{-1}$), PAA ($M_w = 250,000 \text{ g mol}^{-1}$), PSS ($M_w = 200,000 \text{ g mol}^{-1}$), and PEI ($M_w = 750,000 \text{ g mol}^{-1}$), and the model biomolecules, FITC-dextran ($M_w = 250,000 \text{ g mol}^{-1}$) and rhodamine-B-dextran ($M_w = 70,000 \text{ g mol}^{-1}$) were purchased from Aldrich, USA. Amino-dextran ($M_w = 500,000 \text{ g mol}^{-1}$) and BODIPY FL, SE were purchased from Molecular Probes, USA. Each jetting solution was prepared by dissolution of the components in distilled water (reported as percentage of w/v). For the PEO solutions, centrifugation and filtration were performed before use. All other solutions were used without further purification. Detailed properties of the jetting solutions are included as Supplementary Information.

ELECTRIFIED JETTING WITH A SINGLE CAPILLARY

Jetting solutions were stored in a 1-ml syringe (Becton, Dickinson and Company, New Jersey, USA). The flow rate was controlled by a syringe pump (KDS100, KD Scientific, Massachusetts, USA) with a control step size of $10 \mu\text{l h}^{-1}$. A conducting single capillary (Precision stainless steel tips, 21 gauge, 0.5 inch long, EFD, Rhode Island, USA) was connected by the tip of the syringe and further attached to the cathode of the high-voltage supply. The electron voltage was controlled in the range 5–15 kV. A square piece of aluminium foil was connected to the anode as a collecting substrate. For samples examined with the confocal microscope, glass slides were placed on top of the aluminium foil (counter-electrode). In all cases, the distance between the electrodes was adjusted vertically in the range 5–25 cm.

ELECTRIFIED JETTING WITH SIDE-BY-SIDE DUAL CAPILLARIES

The experimental setup for biphasic jetting was similar to that used for single-phase jetting as described above, except for the configuration of the capillary setup, through which the two jetting liquids were fed: using the dual-syringe-applicator assembly (Fibrijet SA-0100, Micromedics, Minnesota, USA), two 1-ml syringes were controlled by a single syringe pump. Each syringe was loaded with a specific jetting solution. The two syringes were connected to a dual-channel tip (Fibrijet SA-0105, Micromedics, Minnesota, USA), which had two capillaries with dimensions of 26 gauge and 3 inch in length. These dual capillaries were covered with a transparent plastic tube that confined the two capillaries in a side-by-side orientation.

CONFOCAL MICROSCOPY

Images were taken with a SP2 confocal laser scanning microscope (Leica, USA) on the substrate containing the nanocolloids. To detect incorporated biomolecules, an Ar/ArKr laser (wavelength 488 nm) and a GreNe laser (wavelength 543 nm) were used to excite FITC-dextran and rhodamine-B-dextran, respectively. The detection wavelength range for each fluorescence emission was confined to 508–523 nm for FITC and 580–595 nm for rhodamine B. The same lasers were used for excitation of BODIPY and rhodamine B during the selective chemical modification experiment. The detection wavelength range for fluorescent emission was confined to 500–535 nm for BODIPY and 570–630 nm for rhodamine B.

ELECTRON MICROSCOPY

TEM images were obtained using a 2010 STEM (JEOL, JAPAN) with an accelerating voltage of 200 kV. All TEM samples were prepared by direct jetting onto a carbon film on top of a copper grid (400 mesh, Ted Pella, Redding California, USA), which was mounted onto the counter-electrode. Scanning electron microscopy (SEM) images were obtained using a XL30 FEG SEM (Philips, USA) at 5 kV. SEM samples were prepared by direct jetting onto a piece of 1 square inch of aluminium foil used as counter-electrode, and were examined by SEM without further coating with a conductive layer.

SIZE-DISTRIBUTION MEASUREMENT

On the basis of the SEM images, bead diameters were determined. For beads with spindle-like shapes, lengths were separately measured both along the main axis and perpendicular to the main axis. The arithmetic mean value of those two diameters was used to obtain the histogram.

SELECTIVE CHEMICAL MODIFICATION

For surface modification, the substrate containing the nanocolloids was immersed in BODIPY dye solution dissolved in *n*-hexane (5 p.p.m.). The succinimidyl ester groups of the dye reacted within 15 min selectively with the amino groups of the particles to form a stable amide bond. After reaction, particles were immersed in excess of clean hexane for 90 min to wash out unreacted dye and then visualized using confocal microscopy.

Received 10 May 2005; accepted 9 August 2005; published 25 September 2005.

References

- Glotzer, S. C. Some assembly required. *Science* **306**, 419–420 (2004).
- Zhang, Z. L. & Glotzer, S. C. Self-assembly of patchy particles. *Nano Lett.* **4**, 1407–1413 (2004).
- Manna, L., Milliron, D. J., Meisel, A., Scher, E. C. & Alivisatos, A. P. Controlled growth of tetrapod-branched inorganic nanocrystals. *Nature Mater.* **2**, 382–385 (2003).
- Malikova, N., Pastoriza-Santos, I., Schierhorn, M., Kotov, N. A. & Liz-Marzan, L. M. Layer-by-layer assembled mixed spherical and planar gold nanoparticles: control of interparticle interactions. *Langmuir* **18**, 3694–3697 (2002).
- Hulvat, J. F. & Stupp, S. I. Anisotropic properties of conducting polymers prepared by liquid crystal templating. *Adv. Mater.* **16**, 589–592 (2004).
- Teranishi, T., Inoue, Y., Oumi, Y. & Sano, T. Nanocones: anisotropically phase-segregated CoPd sulfide nanoparticles. *J. Am. Chem. Soc.* **126**, 9914–9915 (2004).
- Taylor, G. Disintegration of water drops in electric field. *Proc. R. Soc. Lond. A* **280**, 383–397 (1964).
- Zeleny, J. On the conditions of instability of electrified drops, with applications to the electrical discharge from liquid points. *Proc. Camb. Phil. Soc.* **18**, 71–83 (1915).
- Dzenis, Y. Material science: spinning continuous fibres for nanotechnology. *Science* **304**, 1917–1918 (2004).
- Reneker, D. H. & Chun, I. Nanometre diameter fibres of polymer, produced by electrospinning. *Nanotechnology* **7**, 216–223 (1996).
- Fong, H., Chun, I. & Reneker, D. H. Beaded nanofibres formed during electrospinning. *Polymer* **40**, 4585–4592 (1999).
- Jun, Z., Hou, H., Schaper, A., Wendorff, J. H. & Greiner, A. Poly-L-lactide nanofibres by electrospinning—Influence of solution viscosity and electrical conductivity on fiber diameter and fiber morphology. *e-Polymers* **009**, 1–9 (2003).
- Zeng, J. *et al.* Ultrafine fibres electrospun from biodegradable polymers. *J. Appl. Polym. Sci.* **89**, 1085–1092 (2003).
- Sanders, E. H., Kloefkorn, R., Bowlin, G. L., Simpson, D. G. & Wnek, G. E. Two-phase electrospinning from a single electrified jet: microencapsulation of aqueous reservoirs in poly(ethylene-co-vinyl acetate) fibres. *Macromolecules* **36**, 3803–3805 (2003).
- Sun, Z., Zussman, E., Yarin, A. L., Wendorff, J. H. & Greiner, A. Compound core-shell polymer nanofibres by co-electrospinning. *Adv. Mater.* **15**, 1929–1932 (2003).
- Loscertales, I. G. *et al.* Electrically forced coaxial nanojets for one-step hollow nanofiber design. *J. Am. Chem. Soc.* **126**, 5376–5377 (2004).
- Larsen, G., Velarde-Ortiz, R., Minchow, K., Barrero, A. & Loscertales, I. G. A method for making inorganic and hybrid (organic/inorganic) fibres and vesicles with diameters in the submicrometer and micrometer range via sol-gel chemistry and electrically forced liquid jets. *J. Am. Chem. Soc.* **125**, 1154–1155 (2003).
- Loscertales, I. G. *et al.* Micro/nano encapsulation via electrified coaxial liquid jets. *Science* **295**, 1695–1698 (2002).
- Berkland, C., Daniel, W., Pack, D. W. & Kim, K. Controlling surface nano-structure using flow-limited field-injection electrostatic spraying (FFESS) of poly(d,l-lactide-co-glycolide). *Biomaterials* **25**, 5649–5658 (2004).
- Berkland, C., Pollauf, E., Pack, D. W. & Kim, K. Uniform double-walled polymer microspheres of controllable shell thickness. *J. Control. Release* **96**, 101–111 (2004).
- Gupta, P. & Wilkes, G. L. Some investigations on the fiber formation by utilizing a side-by-side bicomponent electrospinning approach. *Polymer* **44**, 6353–6359 (2003).
- Madhugiri, S., Dalton, A., Gutierrez, J., Ferraris, J. P. & Balkus, K. J. Jr. Electrospun MEH-PPV/SBA-15 composite nanofibres using a dual syringe method. *J. Am. Chem. Soc.* **125**, 14531–14538 (2003).
- Barrero, A., Gañán-Calvo, A. M., Dávila, J., Palacio, A. & Gómez-González, E. Low and high Reynolds number flows inside Taylor cones. *Phys. Rev. E* **58**, 7309–7314 (1998).
- <http://www.susqu.edu/facstaff/b/brakke/evolver/evolver.html>.
- Utada, A. S. *et al.* Monodisperse double emulsions generated from a microcapillary device. *Science* **308**, 537–541 (2005).
- Xu, S. *et al.* Generation of monodisperse particles by using microfluidics: control over size, shape, and composition. *Angew. Chem. Int. Edn Engl.* **44**, 724–728 (2005).
- Hermanson, G. T. *Bioconjugate Techniques* (Academic, San Diego, 1995).
- Millman, J. R., Bhatt, K. H., Prevo, B. G. & Velev, O. D. Anisotropic particle synthesis in dielectrically controlled microdroplet reactors. *Nature Mater.* **4**, 98–102 (2005).
- Lu, Y. *et al.* Asymmetric dimers can be formed by dewetting half-shells of gold deposited on the surfaces of spherical oxide colloids. *J. Am. Chem. Soc.* **125**, 12724–12725 (2003).
- Paunov, V. N. & Cayre, O. J. Supraparticles and 'Janus' particles fabricated by replication of particle monolayers at liquid surfaces using a gel trapping technique. *Adv. Mater.* **16**, 788–791 (2004).

Acknowledgements

We thank Solomon, University of Michigan, for use of the confocal laser scanning microscope and Manke, Wayne State University, for use of the viscometer. D.C.M. acknowledges partial support from the National Science Foundation through grant DMR-0084304. Correspondence and requests for materials should be addressed to J.L. Supplementary Information accompanies this paper on www.nature.com/naturematerials.

Competing financial interests

The authors declare that they have no competing financial interests.

Reprints and permission information is available online at <http://npg.nature.com/reprintsandpermissions/>